The role of clustering effects in interpreting nondiffusive transport measurements in tokamaks

J. P. Graves, R. O. Dendy, K. I. Hopcraft, and E. Jakeman

Citation: Phys. Plasmas **9**, 1596 (2002); doi: 10.1063/1.1464148
View online: http://dx.doi.org/10.1063/1.1464148
View Table of Contents: http://pop.aip.org/resource/1/PHPAEN/v9/i5
Published by the American Institute of Physics.

The role of clustering effects in interpreting nondiffusive transport measurements in tokamaks

J. P. Graves[a)]
Theoretical Mechanics Division, School of Mathematical Sciences, University of Nottingham, University Park, Nottingham, NG7 2RD, United Kingdom

R. O. Dendy
EURATOM/UKAEA Fusion Association, Culham Science Centre, Abingdon, OX14 3DB, United Kingdom

K. I. Hopcraft and E. Jakeman
Theoretical Mechanics Division, School of Mathematical Sciences, University of Nottingham, University Park, Nottingham, NG7 2RD, United Kingdom

(Received 13 November 2001; accepted 31 January 2002)

Recent measurements in tokamak plasmas provide clear evidence for rapid nondiffusive transport and non-Gaussian fluctuations, and have been widely interpreted in terms of the sandpile and self-organized criticality (SOC) paradigms. Many of the statistical physics inferences that can be drawn from observations of, for example, avalanching transport remain to be explored. This paper will show that the statistical characterization of both experimentally observed and simulated avalanching transport phenomena reveals several points of contact with existing stochastic process models that have seldom been deployed in a plasma physics context. It will be shown that statistical physics techniques developed to model clustering of events can be used to characterize microscopic fluctuations in both local density and flux, as well as the global transport properties to which they give rise. This provides a fresh interpretation for some of the key aspects of observed critical gradient-driven transport phenomenology in tokamaks. In particular it provides new evidence for scale-free correlations in the fluctuations which drive the transport, and quantifies their distribution in terms of few-parameter non-Gaussian models. The correlation properties of density fluctuations can be interpreted in terms of random walk models, whereas flux fluctuations cannot: instead they can be described by the discrete negative binomial distribution, which again indicates clustering. Some of the spatio–temporal correlations considered emulate multichannel measurements in tokamaks, and it is shown how these can be used to characterize the transport of naturally arising coherent structures. © *2002 American Institute of Physics.* [DOI: 10.1063/1.1464148]

I. INTRODUCTION

The characterization and interpretation of nondiffusive transport and non-Gaussian fluctuation measurements in tokamak plasmas is an important topic in magnetic fusion research. Extensive experimental evidence has been found for avalanching transport in tokamaks,[1,2] while numerical simulations display similar effects.[3–5] In parallel, careful measurement and analysis of edge plasma turbulence in tokamaks (see, for example, Refs. 6–10), has revealed clear evidence for non-Gaussian probability distribution functions (PDFs) that are often long-tailed, and may be inverse power law in certain circumstances. These observations have in turn triggered a number of linked debates on their theoretical interpretation and practical implications, which include the following.

(1) To what extent do the observations[1–10] support the increasing adoption of the sandpile paradigm to describe[11–18] these aspects of anomalous transport in tokamaks?
(2) If the sandpile paradigm is applicable, what are the implications for wider tokamak phenomenology? Links have been drawn with enhanced confinement, edge localized modes (ELMs),[17] and internal transport barriers.[11,18]
(3) To what extent, and in what regions, might some tokamak plasmas be in a state of self-organized criticality (SOC),[19–21] or magnetospheric plasmas?[40,41] And if so, does it matter? For example, a discussion of what can be inferred from long-tailed PDFs in this context is given in Ref. 22, while in Ref. 17 it is argued that L-mode confinement may correspond to SOC.

The sandpile paradigm is attractive because it can model self-regulating, driven-dissipative, nonequilibrium confinement systems that have nonlocal transport arising from local redistribution triggered by critical gradients. Mathematical sandpile cellular automata have few control parameters, and yield reproducible data in sufficient quantity to enable reliable statistical inferences to be drawn. Such data are uncontaminated by instrumental factors, and untroubled by issues such as the absence of guaranteed quasistationarity that can be problematic for tokamak data. Section III of the present paper provides a quantitative account of the close parallels

a)Present address: Centre de Recherches en Physique des Plasmas, Association Euratom–Confédération Suisse, EPFL, CH-1015 Lausanne, Switzerland; electronic mail: jonathan.graves@epfl.ch

that exist between the measurements of edge density fluctuations in the DIII-D tokamak reported in Ref. 10, and the height fluctuations of the sandpile cellular automaton described in Refs. 23 and 24. An important and distinctive feature of the cellular automaton is that it enables the microphysics of the avalanches to be resolved at the level of tracing the motion of individual grains. This paper explores the single interval statistical properties of physically measurable quantities associated with these motions, together with their spatial and temporal correlation properties that are revealed by the application of multichannel measurements. In this respect, the work presented here parallels recent studies of non-Gaussian test particle transport in numerical simulations of strong plasma turbulence.[25,26] This is explored in Sec. III, and furthermore enables multichannel measurements to be obtained; from these, in Sec. IV, are calculated spatio–temporal flux correlations which emulate measurements that can be performed in tokamak plasmas and in numerical simulations thereof.

This paper is primarily concerned with using the concept of clustering as a basis for the statistical characterization of nondiffusive transport behavior in plasmas. In broad terms, clustering is manifested by correlations between observables measured at different times, different locations, or both. Clustering is both a statistical observable and a physical concept: it originates in the underlying physical processes driving the transport, and can be quantified and modelled mathematically. A fundamental message of this paper will be that, once a critical gradient has been exceeded, clustering of transport events is sufficient to generate much of the avalanching phenomenology and non-Gaussian statistical manifestations outlined above. A brief survey of key results on the mathematical physics of clustering is therefore provided in Sec. II.

II. MATHEMATICAL PHYSICS OF CLUSTERING

The purpose of this section is to show that the occurrence of clustering is in itself sufficient to explain many of the non-Gaussian statistics and flicker noise effects observed in sandpiles and, possibly, tokamak transport data, without necessarily invoking SOC. This serves to elucidate what can be inferred about nondiffusive transport processes from the measurement of fluctuations, and to indicate when these can be interpreted in terms of known stochastic models or from properties derived from them. Thus emphasis is placed on the internal microdynamics of systems, their statistical properties and the way that these influence the macroscopic behavior. This approach complements the contrasting methodology that explores non-Gaussian fluctuation phenomena through the concepts of fractional kinetic equations (Ref. 27 and references therein).

A. Power law tails and clustering

The occurrence of probability distributions with power law tails is sometimes cited as evidence of complex or strange kinetic behavior. While this is indeed sometimes the case, it is not necessarily so. The purpose of this section is to review and clarify the circumstances when the occurrence of power law distributions is a characteristic of fractal processes influencing the dynamics, and when their cause can have a less exotic origin.

The growing number of instances of random processes that exhibit scale invariant behavior has caused a resurgence of interest in the class of stable or Lévy probability distributions.[28,29] The Fourier transform of the PDF, or characteristic function, for these distributions has the simple form $C(u)=\exp(-au^{\gamma})$ with a constant and $0<\gamma\leqslant 2$; the Gaussian is a special case corresponding to $\gamma=2$. This form indicates their invariance under convolution, and is the origin of the epithet stable: sums of stable random variables are themselves stable, leading to scale free behavior for random walks whose increments are constructed from them. In general the distributions are characterized by power law tails with $p(x)\sim x^{-1-\gamma}$, so that the variance does not exist.

Both power law behavior and clustering can emerge naturally when characterizing random walks. Consider first Brownian motion, which describes the trajectory $x(t)$ of a particle where the steps in the walk have Gaussian distribution and there is no correlation, or memory, between successive steps. The variance of this stochastic process, or the mean square displacement, increases linearly with time, $\langle x^2\rangle\sim t$. The Hausdorff–Besikovich dimension D (Ref. 30) of such a Brownian trace is 3/2, indicating that it is more convoluted than a line $(D=1)$, but less so than a space filling curve $(D=2)$. The distribution of time intervals τ for the trace to return to its initial location (the return time) is, in this case, exactly a stable distribution,[31]

$$p(\tau)=\frac{1}{\sqrt{2\pi\tau^3}}\exp\left(-\frac{1}{2\tau}\right)$$

with tail $p(\tau)\sim\tau^{-\upsilon}$ where $\upsilon=3/2$. Stable distributed random variables exhibit clustering. For example, consider the return times which correspond to the intervals between zero crossings of a Brownian trace: this crosses infinitely fast in the vicinity of another zero, but conversely the probability of finding a zero crossing in a neighborhood of the trajectory that is distant from the origin is small. Hence the zero crossings appear in clusters, interspersed with long flights. It follows that any physical measurable that can be placed in correspondence with a random walk will necessarily exhibit these statistical properties.

Fractional Brownian motion[32] (FBM) generalizes Brownian motion to a random walk whose increments are Gaussian random variables, but where memory is retained of earlier steps. The structure function for this process is $\langle(x(t)-x(0))^2\rangle\sim t^{2H}$, defining the Hurst exponent[30] which falls in the range $0<H<1$. The Hausdorff–Besikovich dimension of a FBM trace is $D=2-H$, so that $1<D<2$ as required. If $H<1/2$, the motion is anticorrelated (or antipersistent), and $3/2<D<2$ implying that the trace is more convoluted than Brownian motion which corresponds to $H=1/2$. Conversely, $H>1/2$ describes persistent or positively correlated motions with $1<D<3/2$, so that the trace appears to be smoother. The return time distribution for FBM is asymptotically a stable distribution with power law tail of the

form $p(\tau)\sim\tau^{-v}=\tau^{-(2-H)}$. Hence the indices for the return times for FBM are the same as D and fall into the range $1<v<2$.

Recent sandpile simulations[24] have prompted the generalization of FBM to fractional non-Brownian motion (FNBM), which is a correlated random walk with non-Gaussian skewed (i.e., asymmetric) increments which nevertheless have zero mean. The return time distribution for this case is $p(\tau)\sim\tau^{-(2-H-f(s,H))}$ from which an effective Hurst exponent can be identified: $H^*=H+f(s,H)$, where $f(s,H)$ is an even function of the skewness $s=\langle x^3\rangle/\langle x^2\rangle^{3/2}$ of the distribution for the increments. Moreover, $f(s,H)$ is a nonlinear function of the Hurst exponent, being identically zero for $H\geqslant 1/2$ and positive if $H<1/2$. The net effect of the non-Gaussian increments is to decrease the greatest possible value of v from 2, while leaving unaltered the lower bound of unity. Hence return time distributions for these types of motions all have indices $v<2$. This contrasts with sandpile simulations,[24] experiments,[33] and tokamak data[10] which all have indices $v>2$ for quantities that can be interpreted as return time distributions. The apparent paradox was resolved[24] for sandpiles by demonstrating that fluctuations in addition to those described by FNBM modify the dynamics, thereby allowing the regime $v>2$ to be accessed—thus the process is necessarily multiscale in this instance.

B. The negative binomial distributions

Clustering can also be manifested by discrete random variables in population models. In the present context, for example, a birth–death–immigration process[34,35] can be viewed as a naïve description for three-dimensional turbulence, which nevertheless incorporates some of the salient physics. There is spontaneous nucleation or immigration of large eddies, which give birth to smaller eddies, which eventually die through dissipation.[34,35] The equilibrium probability distribution for the occupancy number n (e.g., the number of eddies present at a given time) for this process is the negative binomial distribution[34]

$$P(n)=\binom{n+\alpha-1}{n}\frac{(\overline{n}/\alpha)^n}{(1+\overline{n}/\alpha)^{n+\alpha}}. \tag{1}$$

Here $\overline{n}$ denotes the mean occupancy number and $\alpha\geqslant 0$ is a measure of the degree of clustering, which also determines the normalized second factorial moment (a measure of the variance)

$$n^{[2]}\equiv\frac{\langle n(n-1)\rangle}{\overline{n}^2}=1+\frac{1}{\alpha}. \tag{2}$$

Distributions exhibit clustering insofar as $n^{[2]}$ exceeds unity.[34] Special cases of the negative binomial distribution include $\alpha=1$, which is the geometric (or Bose–Einstein) distribution; when $\alpha\to\infty$, which corresponds to no clustering, it reduces to the Poisson distribution. The negative binomial distribution is perhaps more familiar in the continuum limit, $n\to\overline{n}y$, then $\overline{n}\to\infty$ with y finite. This yields the gamma distribution with density

$$p(y)=\frac{\alpha}{\langle y\rangle\Gamma(\alpha)}\left(\frac{\alpha y}{\langle y\rangle}\right)^{\alpha-1}\exp\left(-\frac{\alpha y}{\langle y\rangle}\right), \tag{3}$$

where $\Gamma(\alpha)$ is the gamma function.[36] It is noteworthy that the distribution of interevent times for the birth–death–immigration process exhibits a regime of power-law behavior[37] with index v which is necessarily greater than 2. Thus the distributions for interevents times and the return times for Brownian motion and all its variants are closely related phenomena, and when these exhibit power-law behavior, the common ingredient is clustering.

It has been found empirically that the discrete negative binomial distribution governs certain features in the temporal behavior of the sandpile[23] and the links to tokamak measurements will be studied here. This paper will show that its significance is more pervasive, for it accurately describes the fluctuations in the flux of grains passing through the pile and approximates the intervals in time between these bursts or mass transfer events.

III. STATISTICS OF DENSITY FLUCTUATION MEASUREMENTS

This section examines the fluctuation properties of the local density of the sandpile, and relates it to specific tokamak measurements. This is achieved by first obtaining the distribution for the times for the density to return to its mean local value, as examined in Ref. 10. This derived property of the density fluctuations contains information about the higher order statistical, or temporal correlation properties. Spatial correlations can also be treated and are considered in Sec. III B. Before embarking on this it is worthwhile recalling the formulation of the sandpile algorithm, which is an extension[23,24] of that introduced in Ref. 38, which was designed to replicate the Oslo ricepile[39] and especially the measurements of tracer grains[33] therein. Unlike most sandpile algorithms, it tracks individual grains as they move through the pile, so that it can play a role analogous to test-particle transport simulations in plasmas. Importantly, this introduces physics on a new time scale, that of grain redistribution. This is shorter than the minimum resolvable timescale, the interval between adding grains to the sandpile, that is permitted in the majority of sandpile algorithms. This feature also enables the application of novel diagnostics which have been used[23,24] to explain the origin of the self-organized behavior that arises. Briefly, the cellular automaton proceeds by testing the stability of a set of gradients z_m, where integer values $1<m<L$ label a spatial position (or cell). The size of the pile $L=400$ here unless stated otherwise, and the sandpile is fueled with grains of unit size at the first cell, so that $z_1\to z_1+1$ at each fueling event. A critical gradient z_m^c with value 1 or 2 is assigned randomly at each cell, and if the local gradient z_m equals or exceeds z_m^c, sand is redistributed according to the rule $z_{m-1}\to z_{m-1}+1$, $z_m\to z_m-2$, $z_{m+1}\to z_{m+1}+1$. Special conditions apply at the final cell of the sandpile $(m=L)$ to allow grains to leave the system, so that if $z_L\geqslant z_L^c$, $z_{L-1}\to z_{L-1}+1$, $z_L\to z_L-1$. The value of z_m^c is reassigned whenever a grain passes the mth cell, and adopts values 1 or 2 with equal probability. The redistribution of

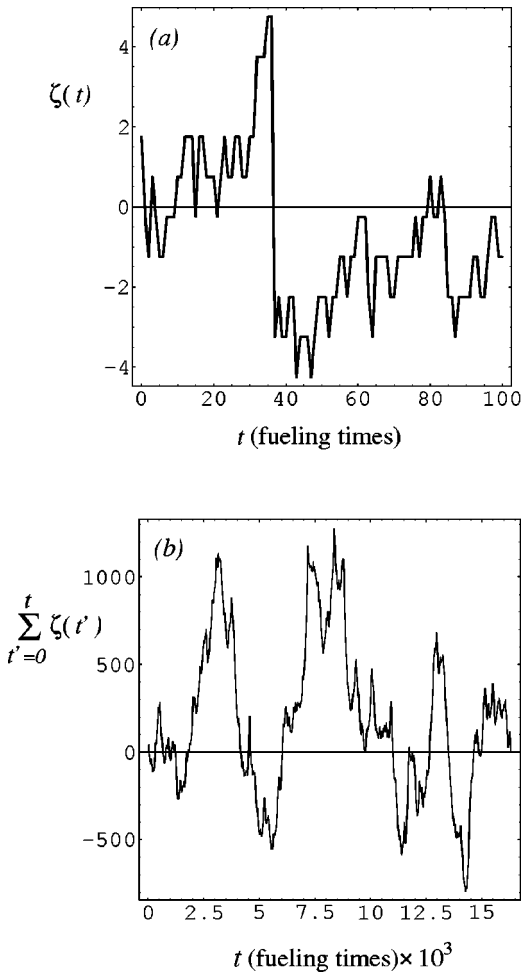

FIG. 1. (a) Time trace of the fluctuations in the height about the mean $\zeta(x,t)=h-\langle h\rangle$ at site 100 in the sandpile where t is measured in fueling times. (b) The time integrated height fluctuations over 15 000 fueling times at the same site in the sandpile. Note the size of the fluctuations in (b) compared to (a) and the fractal characteristics of the traces.

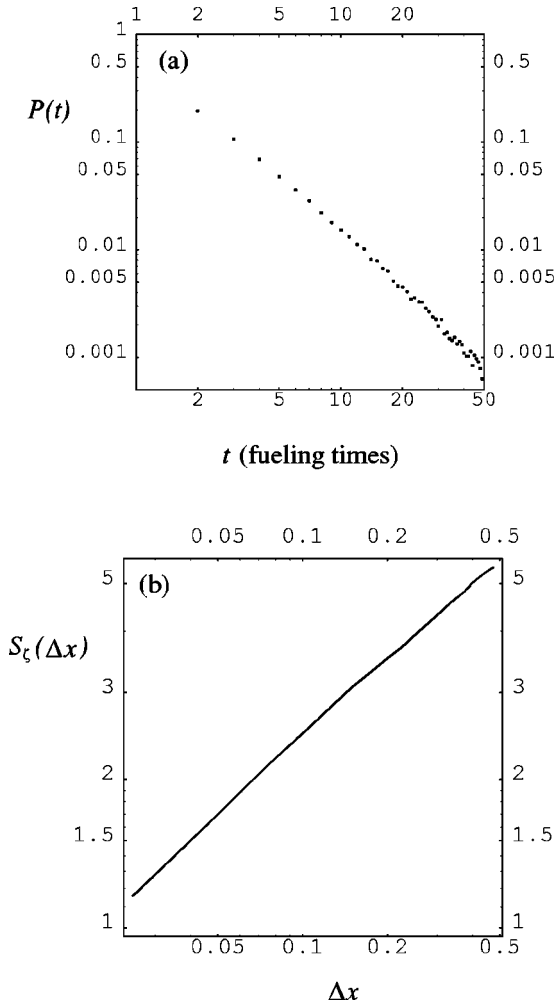

FIG. 2. (a) The probability distribution for the height h to return to its mean value (or ζ to return to zero). It is a power law with $\sim t^{-1.75}$. (b) The spatial structure function which measures the spatial correlation of the height fluctuations. The fractal nature of $S_\zeta(\Delta x)\sim\Delta x^{0.5}$ indicates that the correlation length is the size of the system.

grains at unstable sites occurs sequentially, counting from left to right of the sandpile in accordance with causality. Iteration throughout the sandpile continues until a globally stable state is reached with $z_m \leqslant z_m^c$ everywhere. A further grain is then added at the first cell and the process proceeds.

A. The temporal behavior of the density fluctuations

The configuration of the sandpile can equivalently be described[23,24] in terms of a height distribution $h(x,t)$; here $x=m/L$ represents a normalized cell label. The difference in height between neighboring cells gives the gradient z_m, and t denotes evolution on the fueling time scale. Figure 1(a) shows the height fluctuation $\zeta(x,t)=h(x,t)-\langle h(x)\rangle$ in the sandpile at $x=1/4$, where $\langle h(x)\rangle$ is the local mean height. The result of integrating $\zeta(x,t)$ over time from zero to t' is shown as a function of t' in Fig. 1(b), and is a random walk with wide variation. This quantity is similar in derivation to the integrated local edge density fluctuations in the DIII-D tokamak, shown in Fig. 2(a) of Ref. 10. The data in Fig. 1(a) can be sorted into time intervals where the sign of ζ is constant, and the resulting PDF of the duration of these intervals is shown in Fig. 2(a). This distribution is mathematically equivalent to the distribution of times taken for the height of the sandpile to return to its mean value at the cell in question. On mapping the local height of the pile to local plasma density, this becomes equivalent to the quantity studied in Ref. 10. The distribution shown in Fig. 2(a) exhibits an inverse power law tail with index $v=1.75$. Since this is a distribution for return times, it follows from Sec. II that the effective Hurst exponent $H^*=2-v=0.25$. Furthermore the distribution of increments is non-Gaussian, so that this is equivalent to an antipersistent fractional non-Brownian motion (FNBM). This result is invariant with respect to position x in the sandpile, and to system size L, and is insensitive to box-count averaging.

The index for the return time distribution of the DIII-D edge density fluctuations reported in Ref. 10 is $v=2.4$, and because this exceeds two, implies that processes in addition to FNBM must operate here: for example, multi-time-scale behavior. It has recently been shown[23,24] that indices greater than 2 remain compatible with a sandpile model, provided that it incorporates fluctuations occurring on short intrafueling time scales. Larger values of v correspond to broader

distributions of short time scale events. It is noteworthy that the measured distribution of times for which rice grains remain motionless in the experiment of Ref. 33 also has a power law tail with index $v=2.4(\pm 0.2)$, and a simulation[23] of this experiment yields $v=2.16$. Taken together, the results of this section suggest that the measurements of edge density fluctuations in the DIII-D tokamak reported in Fig. 2(a) of Ref. 10 are entirely compatible with an avalanching paradigm, provided that multiscale dynamics are taken into account.

B. The spatial correlation of density fluctuations–multichannel measurements

Single interval statistics, such as those displayed in Fig. 2(a), can diagnose whether multiscale processes are influencing the evolution. However they cannot describe how that evolution proceeds in space or time. Conversely second order statistics necessarily measure spatio–temporal correlations and the associated occurrence and movement of coherent structures. Both tokamak density and sandpile height profiles are accessible to multichannel diagnostics, which yield information on spatio–temporal behavior and correlation properties. These can be quantified through $S_\zeta(\Delta x)=\langle(\zeta(x,t)-\zeta(x+\Delta x,t))^2\rangle$, the structure function for height fluctuations separated by distance Δx down the pile; here angled brackets denote an ensemble over the fueling time and space. The structure function is linearly related to the autocorrelation function $\rho_\zeta(\Delta x)\sim\langle\zeta(x,t)\zeta(x+\Delta x,t)\rangle$ of the fluctuations in ζ. The reason for using the structure function rather than the autocorrelation function is that it is constructed from the difference between two quantities, so that any long term trends (nonstationarity) in these quantities is subtracted out. Thus, the influence of nonfluctuating quantities, which in general are spatially dependent, is removed. If $S_\zeta(\Delta x)\sim\Delta x^\mu$, this implies that the fluctuations are scale free so that the characteristic correlation length is the size of the system itself. $S_\zeta(\Delta x)$ also measures the roughness of the height profile and so reflects its propensity to instability which is in turn manifested through avalanches. Figure 2(b) shows $S_\zeta(\Delta x)\sim\Delta x^\mu$ with $\mu=0.5$. Furthermore, for FNBM the structure function for the *time* increments is $S_\zeta(\Delta t)\sim\Delta t^{2H^*}$, where H^* denotes the effective Hurst exponent described in Sec. II. By direct calculation of $S_\zeta(\Delta t)$, or by using the inferred value from the return time distribution, it can be shown that the indices for the two structure functions (spatial and temporal) are identical; the implications of this will be discussed in Sec. V. Higher order structure functions have been used recently[25] to characterize the transport of test particles in numerical simulations of resistive pressure-gradient driven turbulence (an example of a critical gradient instability that can generate avalanching transport in plasmas), and the transport was also found to be multiscale in nature.

IV. STATISTICS OF FLUX FLUCTUATION MEASUREMENTS

The fluctuations in the local height of the pile, which here is the proxy for local density fluctuations in a tokamak, are a direct consequence of the movement of grains from other locations. Thus a global variable, namely the flux, affects a local one, the height. Multichannel local flux measurements can be used to quantify the evolution of coherent structures moving across a profile. The statistics for the flux of grains are distinct in character from those of the height fluctuations, which is to be expected for two reasons. First, the quantities evolve on disparate time scales: flux represents the number of grains passing through a region of the pile between consecutive fueling events, and is therefore characterized on the shorter intra-avalanche time scale. Second, fluctuations in the flux cannot be considered as an integrated process and so do not admit an obvious interpretation in terms of random walks. Therefore the concepts of FNBM and return times cannot be applied in this instance.

A. Distribution of flux fluctuations

The empirical probability distribution $P_x(n)$ for the integer number of grains $n>0$ passing though a normalized position $x=m/L$ between successive fueling events is now considered. Recall that most of the pile is in a state of stasis for most of the time, hence the fluctuations are determined only by those events when grain movement occurs, so that $n>0$. A conservation argument requires that on average one grain passes through the pile per fueling time. Furthermore the directionality of the flow from the fueling point to edge necessarily implies that the mean size of avalanches increases with increasing absolute distance down the pile. For the sandpile algorithm used here, the mean flux is measured to scale as $\overline{n}\sim(xL)^{1.2}$. Figures 3(a) and 3(b) show the measured PDF for the number of grains moving through sites 100 and 400, respectively. These flux data can be fitted with remarkable accuracy using the discrete negative binomial distribution of Eq. (1). Figure 3(a) is for site 100, for which the parameters obtained from the data are $\overline{n}=100$ and $\alpha=0.7$, while Fig. 3(b) is for the last site in the pile, where $\overline{n}=516$ and $\alpha=1.78$. These results show that the single interval statistics for the flux of grains depend on position in the pile: the avalanches are progressively larger and marginally less clustered with increasing normalized distance x from the fueling point. However, the class of distribution describing the fluctuations remains negative binomial in both cases, to high accuracy.

The behavior of α with distance x is shown in Fig. 4. The large value of α near the fueling point is indicative of the special conditions that prevail there. Local avalanches are so frequent that there is no opportunity for the pile to establish spatial correlations over any great length, so that the number of moving grains is substantially random, implying a tendency to Poisson statistics. The value of α drops rapidly and then rises more slowly with increasing distance from the fueling point. It is important to note that unlike the mean flux $\overline{n}$, the cluster parameter α depends only on the normalized distance x along the pile and is independent of the system size L. This is a consequence of the measured scaling for the un-normalized second factorial moment $\langle n(n-1)\rangle\sim L^{2.4}$; taken together with the measured scaling $\overline{n}\sim L^{1.2}$ for the mean flux, this implies that the normalized second factorial moment $n^{[2]}\equiv\langle n(n-1)\rangle/\overline{n}^2=1+\alpha^{-1}$ is independent of L.

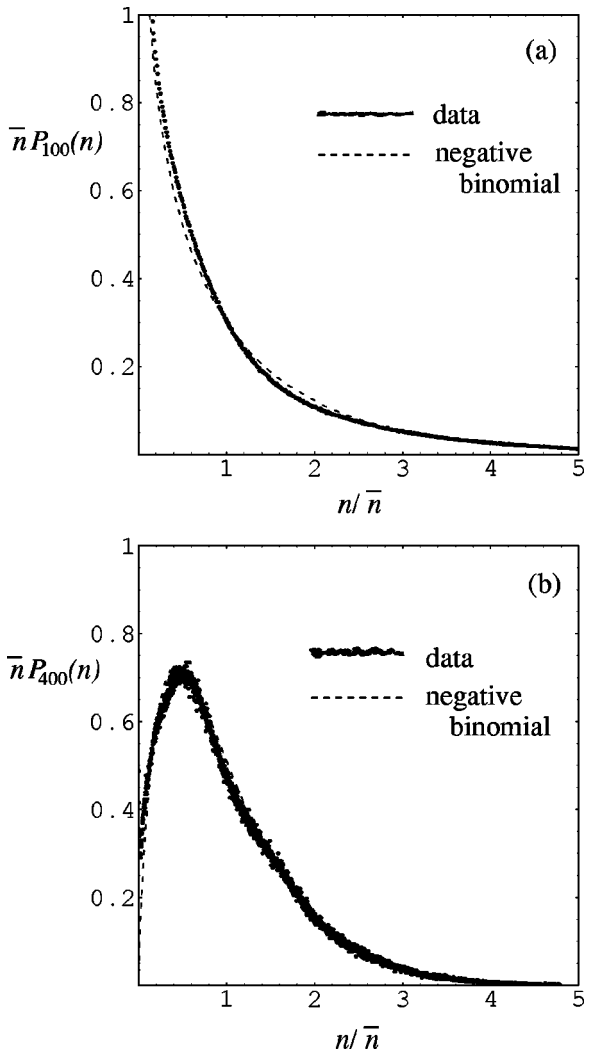

FIG. 3. The probability distribution of the flux of grains and fitted negative binomial distributions [Eq. (1)] for two sites in the sandpile. (a) Site 100 for which the data yields $\bar{n}=100$ and $\alpha=0.71$. (b) Site 400 for which the data yields $\bar{n}=516$ and $\alpha=1.78$.

Regardless of the system size, the cluster parameter is therefore less than 2 at all positions beyond the vicinity of the center of the pile. It is noteworthy that the flux of grains remains strongly clustered at the edge of an arbitrarily large pile. Moreover, since α depends only on distance along the pile relative to the system size, and not simply on the absolute distance, it follows that each location in the pile ''knows'' its position within the system. This observation indicates the mechanism by which the correlated nature of the entire pile is established and maintained. In Ref. 23 it was demonstrated that avalanching grains can only come to rest on plateaux and necessarily traverse sections of staircase. On coming to rest, the grain converts the plateau to a new section of staircase while simultaneously creating a new plateau at one site closer to the fueling point (or alternatively one site further from the edge of the pile). This new plateau is a potential resting place for the next grain participating in the avalanche. Thus one grain prepares the ground for the next; *material* moves down the pile while the *information* that dictates subsequent movements travels in the opposite

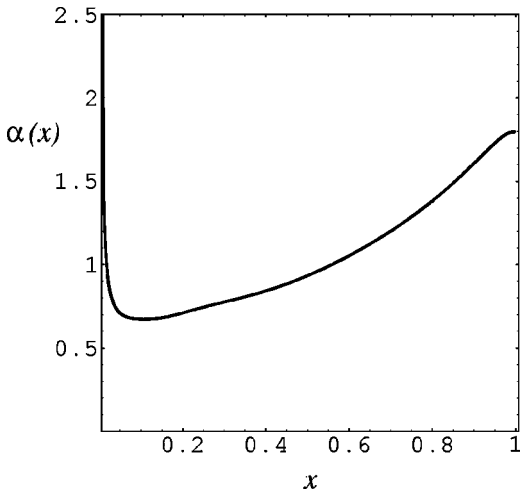

FIG. 4. The spatial dependence of the cluster parameter α for the flux of grains obtained from normalized moments in the sandpile data and plotted as a function of position normalized to sandpile size. Clustering is strongest (low α) just outside the central fueling zone. Clustering declines across the pile but is still large at the edge.

direction. In this respect the behavior is analogous to electrons (grains) and holes (plateaux). To summarize, information in the form of resting positions for avalanching grains moves up the pile in opposition to the flux, thereby continuously ''informing'' each location in the pile of its position relative to the edge, and determining how the fluctuations evolve thereafter.

B. Spatial and temporal behavior of flux events

The degree of spatial coherence of the flux fluctuations can be investigated by constructing the structure function $S_n(\Delta x)=\langle(n(x,t)-n(x+\Delta x,t))^2\rangle$ for the number of grains passing through sites separated by distance Δx. The structure function measures the accumulation or depletion of grains in an interval, and provides a gauge for the compressibility of a moving avalanche. As shown in Fig. 5 it exhibits a fractal structure with $S_n(\Delta x)\sim\Delta x^{1.8}$ and this indicates the correlation length for the flux is, again, the system size. Conversely there is no correlation length shorter than the system size and

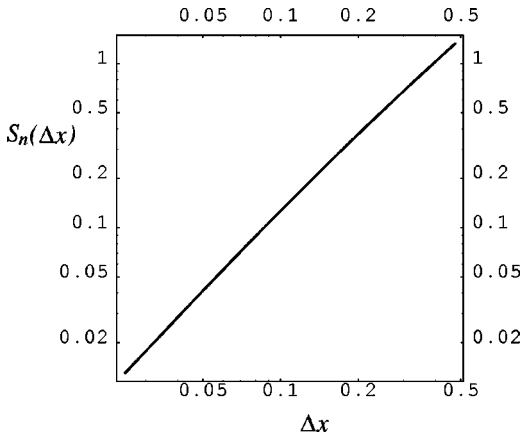

FIG. 5. The spatial structure function which measures the spatial correlation of the flux fluctuations. The fractal nature of $S_n(\Delta x)\sim\Delta x^{1.8}$ indicates that the correlation length is the size of the system.

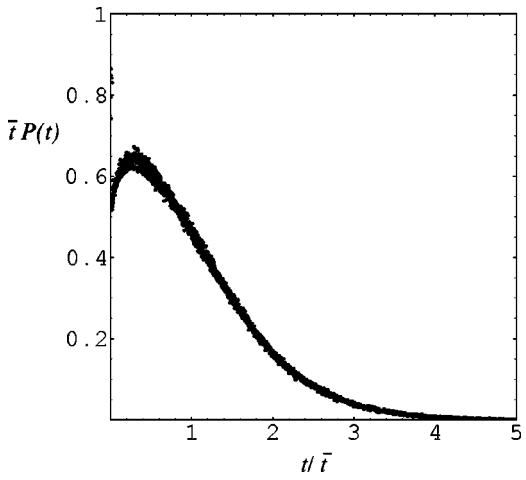

FIG. 6. The probability distribution function $P(t)$ for the time between flux events normalized to the mean interevent time $\bar{t}$. The plot shows data for sites 100, 200, 300, and 400, which have the same distribution upon rescaling with the mean interevent time $\bar{t}$ for each site.

this property is a hallmark of criticality. It may be tempting to relate the index to a Hurst exponent but, as mentioned earlier, the flux is not an integrated process and therefore such an identification is not permitted. However, it is clear that the structure function is scale invariant and the large index corroborates the expected strong spatial correlation within avalanches.

Finally the interevent distribution for times t between avalanches is evaluated. This is a quantity that arises on the fueling time scale and is therefore a discrete random variable. The interval between successive avalanches is recorded irrespective of the size of the avalanches. The mean interevent time is necessarily the same as the mean flux, i.e., $\bar{t}=\bar{n}\sim(xL)^{1.2}$ because of the definition of the fueling time. The size of the flux fluctuations, gauged here by $\bar{n}$, is proportional to the times between flux events, gauged by $\bar{t}$, and can be understood in the following terms. A large avalanche depletes grains from the region of the pile between the fueling point and the location under consideration. This makes that region less steep on average and therefore statistically less susceptible to further avalanches until the region is replenished. Thus the time between large avalanches is correspondingly large, while the converse is true for smaller sized events. Although the value of $\bar{t}$ depends on position, the measured normalized second factorial moment $t^{[2]}=\langle t(t-1)\rangle/\bar{t}^2$ is constant across the entire pile with value $t^{[2]}=1.61$. This again indicates clustering of avalanches, but now in time. Figure 6 shows the interevent time distribution $P(t)$ for sites $m=100$, 200, 300, and 400, thus spanning the whole pile. Upon scaling $t\to t/\bar{t}$ there is complete data collapse over the whole dynamic range. Thus, interevent times are invariant with position and system size, the implications of which will be described in the next section. The distribution which best fits the data is again the negative binomial. Thus the leitmotif of clustering recurs.

V. TRANSPORT OF COHERENT STRUCTURES

Thus far two quantities in the sandpile have been examined separately, namely the height or density fluctuations, and the flux of material. The first is a local variable while the second is not, moreover they evolve on separate time scales. However, the flux fluctuations affect the density fluctuations and lead to the transport of coherent structures in space and time. Empirical evidence for this can be seen in Fig. 7, which shows the evolution of $\zeta(x,t)$ between two global avalanches. It depicts the difference in height of the pile about the local mean value, $\zeta(m,t)=h(m,t)-\langle h(m)\rangle$, as a function of site position m. The different panels show the evolving fluctuations in the profile at the indicated times which are measured on the fueling time scale t, where t increases by one unit per grain added. Note that in Fig. 7 the sites closest to the central fueling point fluctuate most and sites near the edge of the pile least; indeed there are regions towards the end of the pile that remain unaltered between $t=400$ and the global reconfiguration at $t=1601$. The transport down the pile of clusters of material can be seen by comparing consecutive panels. The clusters, boxed in three of the panels of Fig. 7 together with the corresponding cluster of grains from the previous panel (depicted in gray), undergo translation to locations down the pile in such a way that their profile and spatial extent is broadly maintained. If grains are not lost from the edge, the coherent features are also translated in height and the resulting motion is reminiscent of a shelving wave. The region between the central fueling point and site ~ 70 fills up between times $t=1200$ and 1600 (i.e., 400 grains are added), and this has the effect of forming a height profile which has an approximately constant gradient throughout the pile. The next fueling event triggers a global avalanche which substantially depletes the pile of material, leaving heights largely below their mean values. This phenomenology is linked to the equality of indices for the temporal and spatial structure functions for the height fluctuations ζ that was demonstrated in Sec. III, and the reason for this equality can now be understood upon marshalling the following facts. Recall from Sec. III and Ref. 24 that the PDFs for the height fluctuations are invariant with position. A change in height of the pile is caused by the flux of grains from other locations that are closer to the fueling point. Section IV demonstrated that the probability density for the times between consecutive flux events was invariant with position within the pile. These intervals determine the time for a particular cell to change its height. Thus there is a correspondence between a change in height at one location and a change at a different place occurring at a later time. This can be stated mathematically as $\zeta(x-\Delta x,t)\sim\zeta(x,t+\Delta t)$ for suitable increments Δx and Δt, whereupon averaging in space and time, $S_\zeta(\Delta x)=S_\zeta(\Delta t)$ follows immediately. In Sec. III the latter identity was indeed established. This result has the physical interpretation that the height fluctuations are *frozen-in*, giving rise to translation of extended coherent structures through the pile.

VI. DISCUSSION AND CONCLUSIONS

The simple rules that govern the sandpile simulation give rise to a rich phenomenology which displays significant

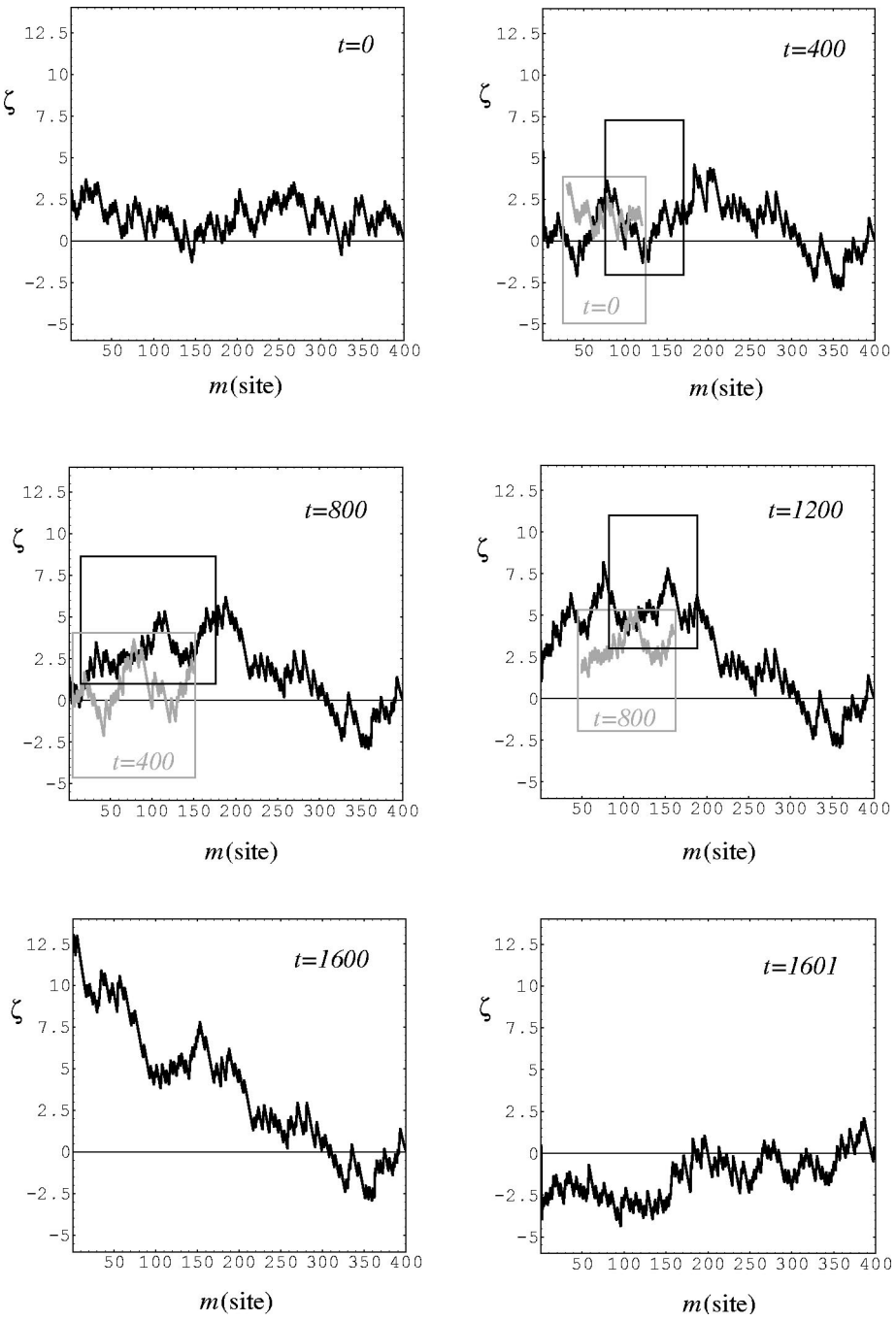

FIG. 7. The height fluctuation ζ at each position in the pile and at times which display the evolution of the profile prior to and just after a major collapse. Inserted boxes highlight coherent structures (apparent clusters of grains) which undergo frozen-in nondiffusive transport down the pile.

points of contact with the fusion plasma data discussed previously. A detailed examination of the microscopic fluctuations that can occur reveals that this diverse behavior can be generated by well-known random processes that are not necessarily associated with SOC or strange kinetics. Diagnostics have been used to describe the spatial and temporal evolution of a density fluctuation measure, together with the flux of material throughout the pile, including the amount of matter leaving it and the distribution of times between mass-transfer events. These investigations have revealed the following issues, all of which are relevant to the physical interpretation of analogous tokamak data.

The spatial correlation properties of the density and flux have fractal structures, implying that no correlation length shorter than the system size exists. These second order statistics yield information on the dynamical evolution of the system, as distinct from single interval statistics whose role is analogous to kinematics. The parameters of the underlying clustering processes are first manifested in the second order statistics, and vestiges of these clustering mechanisms appear as parameters in single interval statistics of specific quantities. Two instances of this are first, the cluster parameter α that uniquely characterizes the structure function $\langle (n(t) - n(0))^2 \rangle$ (Ref. 34) of the population process for which the negative binomial distribution is an equilibrium solution; and second, the index for the power-law tail of the return time distribution that is a function of the Hurst exponent.

The density measurements highlight the importance of

(a) integrated processes such as fractional non-Brownian motion, and (b) multiscale behavior, when interpreting data such as those from DIII-D.[10] The use of Hurst exponents to characterize such data is only appropriate when it can reasonably be argued that the relevant physical process generates a random walk. In the present context, this is appropriate for height or density fluctuations. However flux fluctuations are distinct rather than cumulative events, so that a random walk model is inappropriate. When a Hurst exponent can be assigned, an interpretation can always be made in terms of return times of a random walk. The index of this distribution cannot exceed 2 unless fluctuations on a faster time scale also occur.

The discrete negative binomial distribution evidently underpins different processes in the sandpile that are manifested in measurables that have analogues in tokamak plasmas. For example, the interevent time distributions discussed in Sec. IV B and Ref. 17 have points of contact with the temporal evolution of edge localized modes (ELMs) in tokamaks.

The distribution of times between mass transfer events and fluctuations in density has a functional form which is invariant with position through the pile. Together with the fractal nature of the correlations and their independence of system size, this is sufficient to produce the coherent spatially extended frozen-in fluctuations whose transport is described in Sec. V. These structures may be an analogue for sandpiles of the large-scale long-lived vortices that arise in fluid turbulence models. Evidence of intermittent coherent structures which propagate radially with scale lengths up to the system size have been observed in electron temperature fluctuations of DIII-D.[2] In addition to this, multiple pairwise cross correlation measurements between ECE channels have been used to infer average radial speeds of avalanche-like fluctuations through the tokamak.

Normalized measures of density and flux fluctuations are independent of the sandpile system size. This permits the identification and analysis of invariant statistical properties of the fluctuations, a methodology which can also be applied to tokamak fluctuation measurements. In Ref. 6 the single interval statistics of flux fluctuations were considered by assuming the density and velocity fluctuations to be a joint-Gaussian process with correlation coefficient γ, where $|\gamma|<1$. The PDF for the normalized flux Γ then has the form

$$p(\Gamma)=\frac{(1-\gamma^2)^{1/2}}{\pi}\exp(-\gamma\Gamma)K_0(|\Gamma|),$$

where K_0 is a modified Bessel function. The second normalized moment of these flux fluctuations depends only on the correlation coefficient γ,

$$\Gamma^{[2]}\equiv\frac{\langle\Gamma^2\rangle}{\langle\Gamma\rangle^2}=2+\frac{1}{\gamma^2},$$

so that the minimum value for $\Gamma^{[2]}$ is 3. This may be contrasted with Gaussian fluctuations that have $\Gamma^{[2]}=2$. The relatively high value for the normalized moment stems from the fact that the model allows both positive and negative values of flux to occur, combined with the exponential tails of the PDF. In contrast the sandpile flux is always positive since grains only move down the pile, and the results of Sec. IV show that these fluctuations are, in the continuous limit, accurately described by a gamma random variable. The second normalized moment for these fluctuations is

$$\Gamma^{[2]}=1+\frac{1}{\alpha},$$

where $\alpha\geqslant 0$ is the cluster parameter. The minimum value of the fluctuations in this case is unity, and its smaller value reflects the unidirectionality of the flux. This model clearly enables the regime $1\leqslant\Gamma^{[2]}<3$ to be accessed, indeed the flux fluctuations at the edge of the sandpile have value $\Gamma^{[2]}=1.78$ regardless of the system size. Thus determination of $\Gamma^{[2]}$ from tokamak data, for example, as in Ref. 42 where Joint European Torus (JET) discharges with multichannel measurements show statistically similar flux fluctuations, could facilitate discrimination between models.

In conclusion, the present paper has contributed to augmenting the set of mathematical physics techniques that can be deployed by the fusion research community in addressing the questions (1)–(3) outlined in the Introduction. It was first shown how these techniques can assist the interpretation of a specific set of previously published fluctuation data from the DIII-D tokamak.[10] A well understood sandpile algorithm[23] was used to generate nonlocal, non-Gaussian, and nondiffusive transport phenomenology, as a proxy for a tokamak doing the same. Single-point and two-point statistical analysis of the resulting flux and fluctuation data, using the techniques outlined in Sec. II, yielded new insights into the role of clustering in determining and characterizing similar effects in tokamaks, where equivalent measurements are possible using existing diagnostics. The phenomenology generated by the sandpile algorithm of Ref. 23 includes the spontaneous formation and slow propagation of localized coherent structures in the sandpile profile, which provide a convenient proxy for long lived vortex structures in plasma turbulence. Effective few-parameter characterization of much of the phenomenology is provided by the negative binomial distribution: this provides a mathematically intuitive link to the underlying physical prerequisite—clustering of transport events—and also lends itself naturally to revealing fractal or scale free dynamics.

ACKNOWLEDGMENTS

This work is supported by the United Kingdom Engineering and Physical Sciences Research Council, Euratom, the United Kingdom Department of Trade and Industry, and the Leverhulme Trust.

[1] T. L. Rhodes, R. A. Moyer, R. Groebner, E. J. Doyle, W. A. Peebles, and C. L. Rettig, Phys. Lett. A **253**, 181 (1999).
[2] P. A. Politzer, Phys. Rev. Lett. **84**, 1192 (2000).
[3] X. Garbet and R. Waltz, Phys. Plasmas **5**, 2836 (1998).
[4] Y. Sarazin and P. Ghendrih, Phys. Plasmas **5**, 4214 (1998).
[5] P. Beyer, Y. Sarazin, X. Garbet, P. Ghendrih, and S. Benkadda, Plasma Phys. Controlled Fusion **41**, A757 (1999).
[6] B. A. Carreras, C. Hidalgo, E. Sanchez, M. A. Pedrosa, R. Balbin, I. Garcia-Cortes, B. P. van Milligen, D. E. Newman, and V. E. Lynch, Phys. Plasmas **3**, 2664 (1996).

[7]B. A. Carreras, B. van Milligen, M. A. Pedrosa, R. Balbin, C. Hidalgo, D. E. Newman, E. Sanchez, M. Frances, I. Garcia-Cortes, J. Bleuel, M. Endler, S. Davies, and G. F. Matthews, Phys. Rev. Lett. **80**, 4438 (1998).
[8]B. A. Carreras, B. P. van Milligen, M. A. Pedrosa, R. Balbin, C. Hidalgo, D. E. Newman, E. Sanchez, M. Frances, I. Garcia-Cortes, J. Bleuel, M. Endler, C. Ricardi, S. Davies, G. F. Matthews, E. Martines, V. Antoni, A. Latten, and T. Klinger, Phys. Plasmas **5**, 3632 (1998).
[9]M. A. Pedrosa, C. Hidalgo, B. A. Carreras, R. Balbin, I. Garcia-Cortes, D. Newman, B. van Milligen, E. Sanchez, J. Bleuel, M. Endler, S. Davies, and G. F. Matthews, Phys. Rev. Lett. **82**, 3621 (1999).
[10]G. M. Zaslavsky, M. Edelman, H. Weitzner, B. Carreras, G. McKee, R. Bravenec, and R. Fonk, Phys. Plasmas **7**, 3691 (2000).
[11]D. E. Newman, B. A. Carreras, P. H. Diamond, and T. S. Hahm, Phys. Plasmas **3**, 1858 (1996).
[12]B. A. Carreras, D. Newman, V. E. Lynch, and P. H. Diamond, Phys. Plasmas **3**, 2903 (1996).
[13]B. A. Carreras, D. Newman, V. E. Lynch, and P. H. Diamond, Plasma Phys. Rep. **22**, 740 (1996).
[14]R. O. Dendy and P. Helander, Plasma Phys. Controlled Fusion **39**, 1947 (1997).
[15]S. C. Chapman, R. O. Dendy, and G. Rowlands, Phys. Plasmas **6**, 4169 (1999).
[16]S. C. Chapman, R. O. Dendy, and B. Hnat, Phys. Plasmas **8**, 1969 (2001).
[17]S. C. Chapman, R. O. Dendy, and B. Hnat, Phys. Rev. Lett. **86**, 2814 (2001).
[18]H. R. Hicks and B. A. Carreras, Phys. Plasmas **8**, 3277 (2001).
[19]P. Bak, C. Tang, and K. Wiesenfeld, Phys. Rev. Lett. **59**, 381 (1987).
[20]P. Bak, C. Tang, and K. Wiesenfeld, Phys. Rev. A **38**, 364 (1988).
[21]P. Bak, *How Nature Works* (Oxford University Press, Oxford, 1997).
[22]J. A. Krommes, Phys. Plasmas **7**, 1752 (2000).
[23]K. I. Hopcraft, E. Jakeman, and R. M. J. Tanner, Phys. Rev. E **64**, 016116 (2001).
[24]K. I. Hopcraft, R. M. J. Tanner, E. Jakeman, and J. P. Graves, Phys. Rev. E **64**, 026121 (2001).
[25]B. A. Carreras, V. E. Lynch, and G. M. Zaslavsky, Phys. Plasmas **8**, 5096 (2001).
[26]S. V. Annibaldi, G. Manfredi, and R. O. Dendy, Phys. Plasmas (in press).
[27]B. A. Carreras, V. E. Lynch, D. E. Newman, and G. M. Zaslavsky, Phys. Rev. E **60**, 4770 (1999).
[28]P. Lévy, *Théorie de l'Addition des Variables Aléatoires* (Gauthier-Villars, Paris, 1937).
[29]M. F. Shlesinger, G. M. Zaslavsky, and J. Klafter, Nature (London) **363**, 31 (1993).
[30]P. S. Addison, *Fractals and Chaos: An Illustrated Course* (IOP, Bristol, 1997).
[31]W. Feller, *An Introduction to Probability and Its Applications*, 2nd ed. (Wiley, London, New York, 1971), Vols. I and II.
[32]B. B. Mandelbrot and J. W. van Ness, SIAM Rev. **10**, 422 (1968).
[33]K. Christensen, Á. Corral, V. Frette, J. Feder, and T. Jøssang, Phys. Rev. Lett. **77**, 107 (1996).
[34]E. Jakeman, J. Phys. A **13**, 31 (1980).
[35]E. Jakeman and R. J. A. Tough, Adv. Phys. **37**, 471 (1988).
[36]M. Abramowitz and I. A. Stegun, *Handbook of Mathematical Functions*, 9th ed. (Dover, New York, 1970).
[37]K. I. Hopcraft, E. Jakeman, and R. M. J. Tanner, Phys. Rev. E **60**, 5327 (1999).
[38]M. Boguñá and Á. Corral, Phys. Rev. Lett. **78**, 4950 (1997).
[39]V. Frette, K. Christensen, A. Malthe-Sørenssen, J. Feder, T. Jøssang, and P. Meakin, Nature (London) **379**, 49 (1996).
[40]S. C. Chapman, N. W. Watkins, R. O. Dendy, P. Helander, and G. Rowlands, Geophys. Res. Lett. **25**, 2397 (1998).
[41]A. T. Y. Lui, S. C. Chapman, K. Liou, P. T. Newell, C. I. Meng, M. J. Brittnacher, and G. K. Parks, Geophys. Res. Lett. **27**, 911 (2000).
[42]C. Hidalgo, B. Gonçalves, K. Erents, C. Silva, M. A. Pedrosa, M. Horn, G. F. Matthews, I. García-Cortés, and R. Balbín, "On the radial scale of turbulent transport in the JET plasma boundary region," *Proceedings of the 28th European Conference on Controlled Fusion and Plasma Physics* (European Physical Society, Petit-Lancy, 2001).